university of groningen

University Medical Center Groningen

University of Groningen

(001)-Oriented $Sr:HfO_2$ Ferroelectric Films Deposited by a Flexible Chemical Solution Method

Badillo, Miguel; Taleb, Sepide; Carreno Jimenez, Brenda; Mokabber, Taraneh; Castanedo Pérez, Rebeca; Torres-Delgado, Gerardo; Noheda, Beatriz; Acuautla, Mónica

Published in:
Acs applied electronic materials

DOI:
10.1021/acsaelm.3c01725

IMPORTANT NOTE: You are advised to consult the publisher's version (publisher's PDF) if you wish to cite from it. Please check the document version below.

Document Version
Publisher's PDF, also known as Version of record

Publication date:
2024

Link to publication in University of Groningen/UMCG research database

Citation for published version (APA):
Badillo, M., Taleb, S., Carreno Jimenez, B., Mokabber, T., Castanedo Pérez, R., Torres-Delgado, G., Noheda, B., & Acuautla, M. (2024). (001)-Oriented $Sr:HfO_2$ Ferroelectric Films Deposited by a Flexible Chemical Solution Method. *Acs applied electronic materials*, *6*(3), 1809-1820. https://doi.org/10.1021/acsaelm.3c01725

Copyright
Other than for strictly personal use, it is not permitted to download or to forward/distribute the text or part of it without the consent of the author(s) and/or copyright holder(s), unless the work is under an open content license (like Creative Commons).

The publication may also be distributed here under the terms of Article 25fa of the Dutch Copyright Act, indicated by the “Taverne” license. More information can be found on the University of Groningen website: https://www.rug.nl/library/open-access/self-archiving-pure/taverne-amendment.

Take-down policy
If you believe that this document breaches copyright please contact us providing details, and we will remove access to the work immediately and investigate your claim.

Downloaded from the University of Groningen/UMCG research database (Pure): http://www.rug.nl/research/portal. For technical reasons the number of authors shown on this cover page is limited to 10 maximum.

Download date: 23-06-2024

ACS APPLIED ELECTRONIC MATERIALS

Open Access
This article is licensed under CC-BY 4.0

(001)-Oriented Sr:HfO_2 Ferroelectric Films Deposited by a Flexible Chemical Solution Method

Miguel Badillo, Sepide Taleb, Brenda Carreno Jimenez, Taraneh Mokabber, Rebeca Castanedo Pérez, Gerardo Torres-Delgado, Beatriz Noheda,* and Mónica Acuautla*

Cite This: ACS Appl. Electron. Mater. 2024, 6, 1809−1820 Read Online

ACCESS | Metrics & More | Article Recommendations | Supporting Information

ABSTRACT: Remnant polarization values of ferroelectric HfO_2-based films depend on proper control of the polar orthorhombic phase crystallization and the orientation of the polar domains. Most of the best quality films reported so far are (111)-oriented. While the largest polarization is expected in (001)-oriented films, with the polar axis out of the plane, such orientation is far less common. This paper demonstrates that highly (001)/(010)-oriented heterostructures of Sr:HfO_2 on Pt(111)-buffered Si can be attained in layered films deposited by a recently reported chemical solution deposition route. The oriented films display the short *c*-axis out of plane, giving place to a longer *a* lattice in plane. By tailoring the duration of rapid thermal processing, such oriented films produce highly ferroelectric, leakage-free capacitors. After wake-up cycling, a remnant polarization of 17 $\mu C/cm^2$, which is the highest reported for this dopant and technique, was achieved. Even though optimization is still needed to improve the electrical cyclability, our facile approach produces high-*k*, highly oriented Sr:HfO_2 films, through chemical deposition and annealing, and shows that the crystal orientations and phase purity of HfO_2-based films can be further optimized by cost-effective chemical methods.

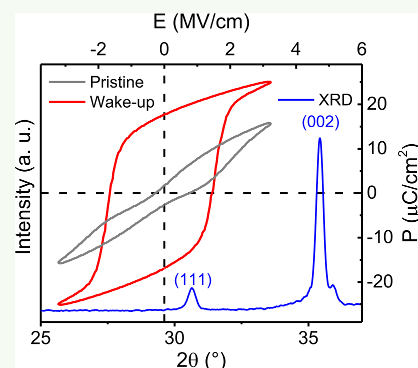

KEYWORDS: *(001)-oriented HfO_2, ferroelectric hafnium oxide, wake-up, phase transition, fatigue*

■ INTRODUCTION

It is now well established that hafnium oxide (HfO_2, hafnia) is a suitable replacement for silicon oxide in silicon-based transistors.[1] The monoclinic phase of HfO_2 is the most stable crystal structure under standard conditions. However, higher symmetry phases, like tetragonal and cubic, can be stabilized under particular processing circumstances.[2] Such phases possess the highest dielectric constants (k) of HfO_2 and are desired for high-k applications. It was during experiments on dielectric control of silicon-doped-hafnia that Böscke et al. observed, for the first time, an unexpected ferroelectric orthorhombic phase.[3] A few years later, an exceptional ferroelectric rhombohedral structure of $Hf_{0.5}Zr_{0.5}O_2$ (HZO),[4] grown epitaxially on $La_{0.7}Sr_{0.3}MnO_3$ (LMSO), was reported by Wei et al.[5] More commonly, however, the orthorhombic structure with space group $Pca2_1$ is deemed as the origin of the remnant polarization (P_r) observed in most HfO_2-based ferroelectrics. Among various mechanisms, the stabilization of polar hafnia can be achieved through crystallite size reduction in very thin films (<10 nm) and by using dopants.[6,7] In particular, the use of dopants brings about the formation of oxygen vacancies, which, when well distributed through the film, help to reduce the energy barrier between different HfO_2 polymorphs.[8] In addition, some research groups have either proven or predicted that some elements are more prone to induce strong ferroelectricity in hafnium oxide. So far, the most promising doping elements for HfO_2 are those of the lanthanide series and those of the alkaline earth metal family, namely, calcium, strontium, and barium (due to high Zr substitution in $Hf_{0.5}Zr_{0.5}O_2$, Zr is not considered a dopant).[9−11]

Thin films grown by strictly controlled methods like pulsed laser deposition (PLD) and atomic layer deposition (ALD) have achieved some of the highest P_r values.[5,12] Usually, a high volume ratio of the orthorhombic phase, compared to other nonpolar phases, is pointed out as the reason for elevated ferroelectricity in HfO_2 films. Interestingly, most reports deal with HfO_2 films of a polycrystalline nature. ALD and PLD methods can sometimes allow for the growth of polar HfO_2 structures with a strong preferential orientation or even fully textured.[13−15] For example, a high remnant polarization of 27.5 $\mu C/cm^2$ in La:HfO_2 films deposited by ALD has been explained by Schenk et al. to originate on a (001) fiber texture of the orthorhombic phase, where the *c*-axis is the polar axis and grows out of plane.[9,12] This can vastly increase P_r by

Received: December 7, 2023
Revised: February 10, 2024
Accepted: February 29, 2024
Published: March 12, 2024

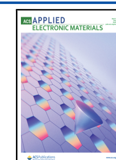

Downloaded via UNIV GRONINGEN on May 17, 2024 at 09:02:44 (UTC).
See https://pubs.acs.org/sharingguidelines for options on how to legitimately share published articles.

ACS Publications
© 2024 The Authors. Published by American Chemical Society

https://doi.org/10.1021/acsaelm.3c01725
ACS Appl. Electron. Mater. 2024, 6, 1809−1820

allowing effective application of the electric field in the direction of polarization of the orthorhombic phase and also by having the participation of a more significant number of ferroelectric domains.[16] It is therefore essential to achieve phase control in HfO_2 and reasonable texture control.

Chemical solution deposition (CSD) methods, which can be regarded as more cost-effective, have been less successful at controlling the orientation of HfO_2-based ferroelectric films. Frequently, due to high thickness-per-layer ratios, HfO_2 films made by CSD grow with a powder-like random distribution of crystalline grains, thus displaying lower ferroelectric performances. Nonetheless, in 2021, Schenk et al. showed that liquid-based methods can also produce HfO_2 ferroelectrics with at least some partial preferential orientation.[17] Using a layer-by-layer crystallization approach (with 5 nm thickness for each layer), they were able to obtain thick La:HfO_2 films (100 nm) with a semipreferential orientation of the orthorhombic phase along the (111) and (001) out-of-plane directions. As they showed, the enhanced proportion of (001)-oriented crystallites doubled the P_r compared to nonoptimized, polycrystalline films. Despite these promising results, highly oriented HfO_2 ferroelectric films fabricated by CSD that can compete with ALD-deposited films are yet to be achieved.

Recently, we reported on a new low-toxicity chemical route for easy fabrication of high-quality, low-leakage, ferroelectric-doped HfO_2 films.[18] For the present study, we have employed a similar approach to produce (001)-oriented Sr:HfO_2 films of 40 nm on Pt-buffered SiO_2/Si with remnant polarization values as large as P_r of 17.3 $\mu C/cm^2$ after wake-up. The obtained polarization values are significantly higher than previously reported in Sr:HfO_2 by CSD.[6,19−21] Larger polarization values have been achieved by CSD only in the work of Starschich et al. for Y:HfO_2 with effective P_r = 20 $\mu C/cm^2$.[22] Yet, in the present case, the films are synthesized by employing a flexible CSD route using stable and less toxic precursors.[18] We propose that our facile chemical approach, along with the use of some other promising dopants such as La and Y, could improve remnant polarization values by controlling crystal orientations in HfO_2-based films and produce thick ferroelectric films that are fully competitive with those deposited by other techniques.[23]

■ EXPERIMENTAL DETAILS

Precursor Solution and Fabrication of Capacitors. A low-toxicity, chemical route for the fabrication of doped HfO_2 was introduced recently by us.[18] In contrast to other CSD existing methods, our approach allows for the use of alcoholic solvents and additives. The same route was employed to prepare a Sr:HfO_2 precursor solution with a doping level of 7.5 at. % of Sr in HfO_2. Consistently, a similar concentration of 7.05 at. % was determined by inductively coupled plasma (ICP) compositional measurements. The targeted concentration of Sr = 7.5 at. % was decided based on the maximum P_r found by Starschich and Boettger for Sr:HfO_2 films.[6] A corresponding small amount of Sr 2,4-pentanedionate salt was incorporated into a blend of isopropyl alcohol, lactic acid, and triethylamine. Hf 2,4-pentanedionate was later added to the mixture. Almost complete dissolution of the solid occurred at room temperature. Still, to ensure an utterly homogeneous precursor, the solution was brought to boil in a round flask with reflux for 4 h at a maximum of 100 °C. The mixture was filtered two times with Whatman filters of 0.2 μm pore size and stored in brown-tinted glass containers, where it can remain stable for up to a year at room temperature.

Thin films of Sr:HfO_2 were deposited by spin-coating 10−20 μL of precursor solution on Pt(111)/Ti/SiO_2/Si substrates of 8 × 8 mm at 4000 rpm for 40 s. After coating, the substrate was put on a hot plate for 5 min at 150 °C to evaporate the solvents. Then, it was moved to a hot plate at 300 °C for another 5 min to allow the pyrolysis of the precursors. Before the deposition of a new layer, the coatings were exposed to UV/ozone cleaning for 5 min. Several films of three layers each were prepared in this way. The resulting Sr:HfO_2 samples were divided into three groups and annealed at a temperature of 800 °C for 60, 90, or 120 s with a rapid thermal annealing (RTA) system. The RTA equipment was own fabricated.[18,24] A batch of 0.5 atm of Ar/O_2 (1:1) was administered during the thermal processing. Metal−insulator−metal (MIM) capacitors were completed by adding top Pt electrodes to the Sr:HfO_2 films. The top Pt was deposited by e-beam evaporation on lithography-patterned Sr:HfO_2. The thickness of the top Pt was 60 nm, and the whole stack was heated at 100 °C for 5 min to improve electrode adhesion.

Materials Characterization. A Rigaku SmartLab XE X-ray diffractometer (XRD) was used for structural analysis. Specular θ−2θ measurements were made in parallel-beam geometry, for which the Si(004) reflection was used as an alignment reference. The same system was also utilized for so-called grazing incidence (GI)-XRD measurements (ω−2θ scans at fixed ω-incident grazing angles) at various ω-angles. Furthermore, fully in-plane XRD measurements ($2\theta\chi$−φ) at a fixed ω-incident grazing angle of 0.5° were made to calculate in-plane lattice parameters. Also, polar figures for (002) and (111) planes of the cubic/tetragonal phase were collected by the Schulz reflection method. The corresponding 2θ angles were fixed, while α (angle away from the surface normal) and β (angle around the surface normal) were scanned.[25] To decrease noise coming from continuous Bremsstrahlung radiation, the background was subtracted by using the signal of a platinized silicon substrate without a HfO_2 layer as a reference. For structural identification, ICDD PDF cards 00-034-0104 (monoclinic HfO_2), 04-002-0037 (cubic HfO_2), 04-011-8820 (tetragonal HfO_2), and 04-005-5597 (orthorhombic HfO_2) were used. In addition, the thickness of the Sr:HfO_2 full layer was measured to be 40 nm by X-ray reflectivity. An aixACCT TF analyzer 2000 was used for ferroelectric and fatigue measurements. Sr:HfO_2 films were measured in the pristine state via the top Pt electrode (circular pads of 50, 75, or 100 μm radius), followed by wake-up cycling and measurement at 1 kHz with the application of 10^3 to 10^4 bipolar rectangular pulses of 3.75 MV/cm in amplitude. Fatigue testing after initial wake-up was made at frequencies 1, 10, 50, and 100 kHz under the same electrical load. Because of the good electrical quality of the Sr:HfO_2 microcapacitors, the dynamic hysteresis measurement (DHM) protocol with triangular pulses was enough to determine ferroelectric properties effectively. The same ferroelectric testing system was used for capacitance−voltage measurements (CVM). A small AC signal of 100 mV and 5 kHz was added to a staircase DC signal with a maximum amplitude of ±10 V. To gather reliable data, we used 500 steps and a relatively long integration time (almost 2 min measurement for each CVM loop). Dielectric constants were calculated from the assumption of a perfect parallel plate capacitor.

■ RESULTS AND DISCUSSION

Highly Ferroelectric Sr:HfO_2 Films by a Simple Chemical Deposition Method. Sr:HfO_2 capacitors of 100 μm in diameter were exposed to wake-up cycling with rectangular pulses of 3.75 MV/cm at 1 kHz for either 10^4 (films annealed for 60 and 120 s) or 10^3 (films with 90 s of annealing) cycles. Dynamic hysteresis measurements were made right after with triangular pulses of 3.25 MV/cm. In Figure 1a, polarization loops are presented for Sr:HfO_2 films annealed at 800 °C for 60, 90, or 120 s. Corresponding transient current density loops, from which polarization loops are built, are shown in Figure 1b. An average remnant polarization (P_r) of 17.3 $\mu C/cm^2$ is obtained with an annealing time of 60 s. The ferroelectric loop is clearly saturated, resulting from strong switching currents with coercive fields of

https://doi.org/10.1021/acsaelm.3c01725
ACS Appl. Electron. Mater. 2024, 6, 1809−1820

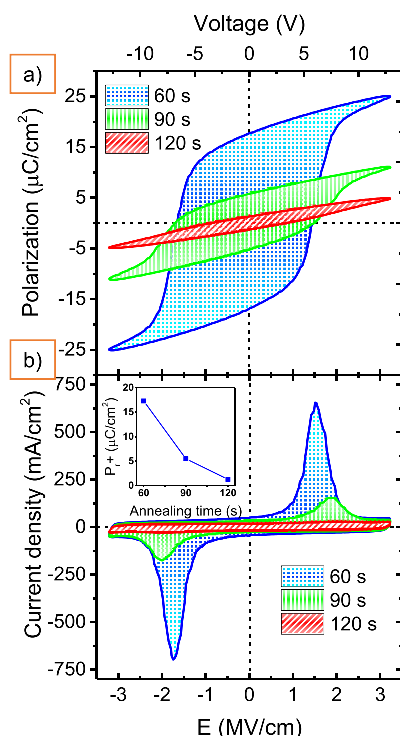

Figure 1. (a) Ferroelectric polarization loop and (b) switching current density response of $Sr:HfO_2$ films annealed at 800 °C for 60 (blue), 90 (green), or 120 s (red), after wake-up cycling and measurement at 1 kHz. Inset in (b) depicts the effect of annealing time on positive remnant polarization. To achieve the maximum ferroelectric response for each sample, the number of fatigue cycles for films annealed for 60 and 120 s was 10^4, while they were 10^3 for the sample annealed for 90 s.

−1.74 and +1.5 MV/cm, and provides evidence of negligible leakage.[26] An annealing time of 90 s produced a strongly reduced remnant polarization for $Sr:HfO_2$ of 5.5 $\mu C/cm^2$, with increased coercive fields of −2.0 and +1.85 MV/cm. A final annealing time of 120 s for $Sr:HfO_2$ gave almost no evidence of switching currents, and thus, the sample behaves mainly as a dielectric material. Therefore, as shown in the inset of Figure 1b, there is a strongly nonlinear increase of the polarization with decreasing annealing times, and it is expected that larger polarizations and smaller coercive fields can still be achieved at shorter annealing times. In our previous work on 5 at. % Ca-doped HfO_2, the maximum remnant polarization was obtained at 800 °C and 90 s of annealing.[18] These annealing conditions are also commonly reported for other CSD-derived HfO_2 films for similar and thicker thicknesses.[6,17,22] For the present $Sr:HfO_2$ films with doping of 7.5 at. %, the lower time of 60 s might be related to the difference in doping levels and smaller thickness (54 vs 40 nm, respectively). It is also known, however, that some dopants, like Sr, make HfO_2 more sensitive to heat treatment.[27] Independently of the specific dopant, these results show the key role of controlling the annealing times for the stabilization of the polar phase of HfO_2 (inset in Figure 1b). Still, considering the role of the kind of dopant, we believe that it is possible to improve the ferroelectric response further by shortening the annealing times.

The maximum apparent P_r of 17.3 $\mu C/cm^2$ of our sample annealed for 60 s is already the highest remnant value reported for $Sr:HfO_2$ films fabricated by chemical solution deposition.[6,19−21] Moreover, it is worth to point out that the observed P_r can be overestimated if the hysteresis loop is rounded by leakage.[26] Therefore, when considering well-saturated ferroelectric loops with low leakage (the "squareness" of the loops) for HfO_2-based films by CSD, our $Sr:HfO_2$ samples have one of the highest P_r reported in the literature, with only $Y:HfO_2$ showing larger P_r = 20 $\mu C/cm^2$.[22] In the sections ahead, we investigate our films further to obtain an insight into the origin of this behavior.

Growth and Orientation of Crystalline Phases after Rapid Thermal Annealing. $Sr:HfO_2$ films deposited by our precursor solution and pyrolyzed in air at 300 °C are amorphous. Subsequently, they are crystallized by rapid thermal annealing at 800 °C for 60, 90, or 120 s. Figure 2 shows out-of-plane X-ray diffraction measurements for a limited 2θ range between 15 and 45°. A small angle offset for the sample of ω = 3° with respect to the incident beam was used to eliminate monocrystalline Si(100)-related reflections. In the linear scale, the diffractogram has been augmented around planes expected for HfO_2. The intense reflection at 39.95° corresponds to Pt(111) on the $Ti/SiO_2/Si$ substrate. As determined from full out-of-plane XRD measurements (Supporting Information), Pt is highly oriented along the (111) direction. The X-ray diffraction measurements were made without a $k\beta$ filter. Thus, the relatively small reflection found at 35.9° is due to the $k\beta$ reflection of Pt(111). Apart

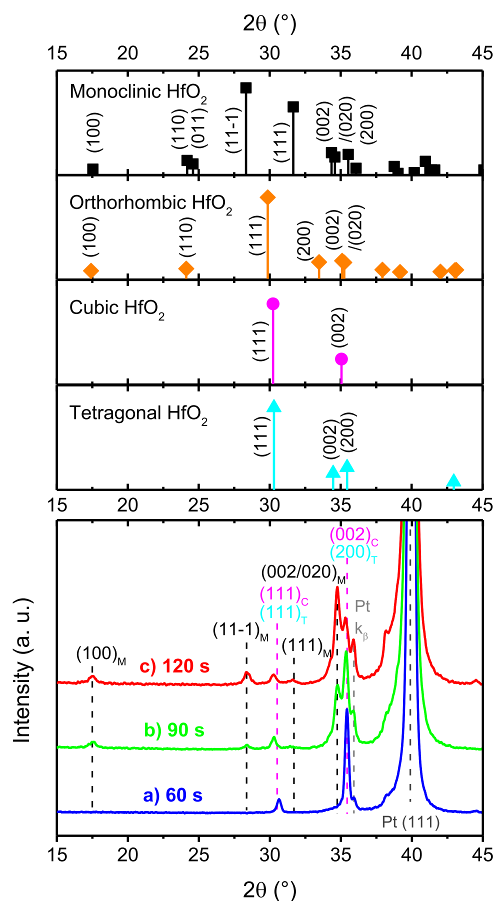

Figure 2. Standard X-ray reflections for powdered HfO_2 of monoclinic, orthorhombic, cubic, and tetragonal phase (up). Out-of-plane θ−2θ X-ray diffraction measurements (down) with an ω angle of 3° for $Sr:HfO_2$ samples annealed at 800 °C for (a) 60 (in blue), (b) 90 (green), and (c) 120 s (red).

from that, all other reflections to the left of Pt(111) correspond to different crystalline structures of HfO_2. For Sr:HfO_2 films annealed for 60 s, only $(111)_C$ of cubic (C-) or $(111)_T$ of tetragonal (T-) is visible at 30.7° and at 35.4° {002} family planes of cubic or $(200)_T$ of tetragonal are found. The possibility of $(002)_T$ of tetragonal, which should appear slightly before 35°, thus indicating a long out-of-plane *c*-axis (Table 1a), has been excluded. Because of the similarity in their interplanar distances, a definitive identification of cubic or tetragonal phases is rather complicated. Moreover, the polar orthorhombic (O-) phase of HfO_2 also shares comparable interplanar distances, thus overlapping with some reflections of the cubic and tetragonal phases. However, the lack of $(100)_O$ and $(110)_O$ planes at around 17 and 24° in Figure 2a (blue), possibly rules out (or indicates in small amounts) the presence of an O-structure.[12] The most striking feature is that a high preferential out-of-plane orientation is observed for HfO_2 along the $[001]_C$ direction of the C-phase or the $[100]_T$ direction of the T-phase. In polycrystalline HfO_2, the $(111)_C$/$(111)_T$ reflection of the C-/T-phase is by far the most intense. Even though the $(111)_C/(111)_T$ plane is also observed in Figure 2a at ≈30.7°, it is weak compared to the other reflections. This suggests a preferential $(001)_C/(100)_T$ orientation of the films. Nevertheless, there is also still a small fraction of randomly oriented grains.

Table 1. (a) Literature-Based Lattice Parameters for HfO_2 Polymorphs, (b) Estimated Out-of-Plane, and (c) Estimated In-Plane Lattice Spacings of Sr:HfO_2 Films Obtained at Various Annealing Times at 800 °C[a]

(a) crystal system			
	a (Å)	*b* (Å)	*c* (Å)
cubic[28]	5.08		
tetragonal[29]	5.06		5.20
monoclinic[30]	5.07	5.14	5.29
polar orthorhombic[31]	5.22	5.02	5.04
(b) out-of-plane lattice parameters			
annealing time (s)	*a* (Å) C-/T-	*b* (Å) M-	*c* (Å) M-
60	<u>5.07</u>		
90	<u>5.07</u>	<u>5.16</u>	5.23
120	<u>5.08</u>	<u>5.16</u>	5.23
(c) in-plane lattice parameters			
annealing time (s)	*a* or *c* (Å) C-/T-	*b* (Å) M-	*c* (Å) M-
60	<u>5.15</u>		
90	<u>5.09</u>	5.22	<u>5.29</u>
120	<u>5.09</u>	5.23	<u>5.30</u>

[a]C-, T-, and M- stand for cubic, tetragonal, and monoclinic phase. Underlined values indicate the preferred axis in either the out-of-plane or in-plane configuration. Due to the mixture of C-/T- and M-phases for samples annealed for 90 and 120 s, *a* of C-/T-phase and *b* and *c* of M-phase were calculated from geometrical considerations. In most cases, interplanar distances of {200} planes were multiplied by two. However, for *c* of M-phase, an angle of 99.3° was considered between *c* and the *ab* plane. From the in-plane configuration, *a*/*c* of C-/T-phase and *b* and *c* of M-phase were also estimated.

Further confirmation of growth in a preferential orientation comes from the phase transformation to the M-HfO_2 phase at longer annealing times. In Figure 2b (green), a few more reflections appear for the annealing of Sr:HfO_2 at 800 °C for 90 s. Although low in intensity, the planes appearing at 17.5 and 30.3° can be identified as the $(100)_M$ and $(-111)_M$ reflections of the M-phase of HfO_2. Interestingly, the reflection at 34.7° can be assigned to the (002/020) planes of the M-phase with high orientation. For an even longer annealing time of 120 s (Figure 2c in red), the $(100)_M$ and $(-111)_M$ reflections become stronger. Remarkably, the $(002/020)_M$ reflection of the monoclinic phase becomes predominant at 120 s of annealing, evidencing also a highly preferential orientation out of plane. In addition, the phase transformation from the $(001)_C/(100)_T$-oriented C-/T- to M-phase with annealing time gives rise almost exclusively to a (001/010) orientation of the M-phase. A slight increase of the (200) reflection of the M-phase at 36° is also observed, but it is not possible to separate it from the $k\beta$ of Pt(111).

Additional evidence of preferential orientation was obtained with GI-XRD. For this, 2θ intensity was collected, while the fixed incident angle (ω) was varied in different scans from 0.55 to 10°. While specular reflections show the grains with atomic planes oriented parallel to those of the substrate, GI-XRD shows those grains that have atomic planes oriented differently from those of the substrate. Since this is the common situation in polycrystalline HfO_2 thin films, this geometry is the one commonly reported in the literature. For a Sr:HfO_2 sample annealed for 60 s, Figure 3a shows the characteristic reflections of the C- and/or T-phase at ω = 0.55°. Nevertheless, a reflection at 60.4°, corresponding to $\{113\}_{C,T}$, can be seen with an abnormally higher intensity than expected for randomly oriented HfO_2 crystals. Although we did not elaborate further in our previous work, this was also found for Ca:HfO_2 films.[18] The reflection at 60.4° becomes more intense as ω increases to 3 and 5°, but it is reduced sharply for higher angles. This indicates a preferential orientation at an inclination away from the surface in the normal direction. Interestingly, the $(002)_C$/$(200)_T$ reflection is weak at ω = 0.55°, but it increases above the intensity of the $(111)_C/(111)_T$ reflection for higher values of ω (going from semi-in-plane to semi-out-of-plane measurement geometry). As shown before in Figure 2a, the $(002)_C$/$(200)_T$ reflection is predominant, meaning a highly preferred $(001)_C/(100)_T$ orientation out of plane.[9] The analysis also holds true for a pristine O-phase with (001)/(010) orientation, which shares diffraction positions with C- and T-phases. In the ferroelectric O-phase, the polar axis is along *c*; yet, the longest lattice parameter in the unit cell is *a* and the *b* lattice parameter is the shortest in the cell (*a* = 5.23 Å, *b* = 5.04 Å, and *c* = 5.06 Å).[31] Nevertheless, it is difficult to unequivocally establish the presence of the polar O-phase. This because the $(100)_O$ and $(110)_O$ reflections do not clearly appear for the Sr:HfO_2 film with 60 s of annealing at 800 °C. They appear, however, for longer annealing times, where the complexity of analysis increases due to the growth of the M-phase. Unfortunately, the M-phase shares the $(100)_M$, $(110)_M$, and several other refraction planes with the O-phase, and thus, it is not possible to resolve them easily. Still, GI-XRD measurements also confirm that a preferential orientation is maintained and that the oriented M-phase grows from the oriented C-/T-/O-phase. For ease of analysis, even though the O-phase might be mixed with C-/T-/M-phases in pristine Sr:HfO_2 samples, in our coming discussion, we will mainly refer to C-/T-/M-phases before wake-up cycling only.

As can be seen in Figure 3b, for 90 s of annealing, a mixture of diffracting planes for C-/T- and M-phases at ω = 0.55° is found. Yet again, the trend for $(002)_C/(200)_T$ is to increase in intensity above that of $(111)_C/(111)_T$ as ω rises. Due to the growth of the M-phase, the corresponding reflection of C-/T-

https://doi.org/10.1021/acsaelm.3c01725
ACS Appl. Electron. Mater. 2024, 6, 1809−1820

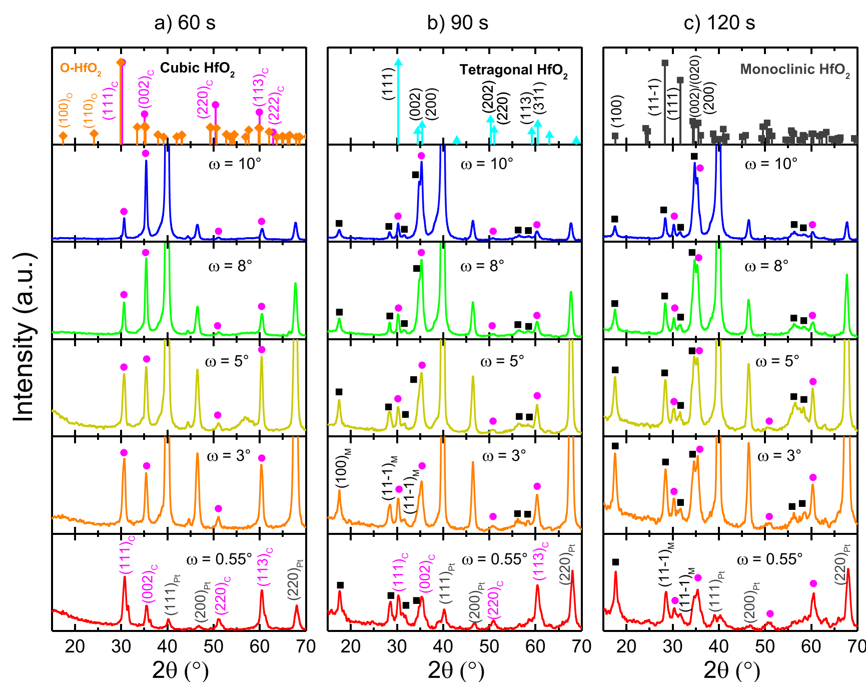

Figure 3. Grazing incidence X-ray diffraction measurements at increasing ω angles for Sr:HfO_2 samples annealed at 800 °C for (a) 60, (b) 90, and (c) 120 s. Standard powder XRD reflections of various HfO_2 polymorphs are added on top for comparison; O-HfO_2 accounts for the orthorhombic phase.

phase HfO_2 observed at 35.4° is accompanied by another reflection at 34.7°. Such a reflection has already been ascribed to $(002/020)_M$. This reflection shows the same directional behavior as the respective $(002)_C/(200)_T$, indicating preferred $(001/010)_M$ orientation out of plane. Further support of the hypothesis is the preference of the $(100)_M$ reflection (2θ = 17°) at low ω angles, which suggests a $(100)_M$ orientation in plane. This is, thus, another evidence that the oriented M-phase is growing from highly oriented C-/T-phase. Calculation of the interplanar distances gives a value of 2.536 Å for $(002)_C/(200)_T$ and 2.580 Å for $(002/020)_M$. Therefore, during annealing, the transformation of C-/T- to M-phase gives rise mainly to an out-of-plane expansion. Yet, due to the increase in the length of both b and c of the M-phase, an in-plane expansion of the cell, which can produce some degree of in-plane strain, is also expected (Table 1b). Accordingly, we also measured our Sr:HfO_2 films in a fully in-plane configuration.

In Figure 4, in-plane XRD measurements show semi-randomly oriented Sr:HfO_2 films. This is in comparison to out-of-plane analysis of Figure 2, more reflections appear (as in polycrystalline films); nonetheless, abnormal intensities of various reflections confirm semipreferential orientations in plane. Figure 4a shows $(200)_C/(002)_T$ and $\{220\}_{C,T}$ reflections of Sr:HfO_2, with 60 s of annealing, at around 35 and 50° in a semipreferred in-plane orientation, respectively. Yet, evidence of $(111)_C/(111)_T$ near 30° is also found, which is due to a fraction of the crystallites following a random orientation (also observed in Figure 2). For Sr:HfO_2 films annealed for 90 and 120 s (Figure 4b,c), an obvious separation of reflections near 35° support the growth of the M-phase with $(002)_M$ and $(200)_M$ semipreferential orientation. It must be considered, however, that mixtures with $(200)_C/(002)_T$ are most likely, as suggested by the presence of $(111)_C/(111)_T$ in Figure 4b,c. An analogous conclusion was supported by out-of-plane and GI-XRD measurements (we further verified it with composition estimations). We also performed calculations of in-plane lattice parameters, which are shown in Table 1c. Our hypothesis of in-plane strain was confirmed by the presence of longer interplanar distances in plane compared to out of plane. Interestingly, for Sr:HfO_2 annealed for 60 s, the estimated a/c lattice parameter of C-/T-phase is 5.15 Å. Such a value is larger than out-of-plane a of C-phase but lower than c of T-phase as reported in the literature (Table 1c,a, respectively). Certainly, the longer in-plane interplanar distance provides evidence of a strained cell. However, the peaks are narrow, which is more indicative of cubic-HfO_2. Expectedly, the tetragonal phase should produce a division of peaks or wider ones. According to theoretical calculations by Yuan et al., the cubic phase of HfO_2 is dynamically unstable at room temperature and it can lead to a cubic-to-tetragonal phase transition.[32] Thus, we believe that our Sr:HfO_2 films annealed for 60 s might be crystallized into a mixture of biaxially strained T-phase and tetragonally distorted C-phase structures. In a later section, we support this idea with dielectric constant measurements.

In the case of Sr:HfO_2 films annealed at 800 °C for 90 and 120 s, the separation of peaks around 35° becomes evident. Estimation of in-plane lattice parameters yields a short a = 5.09 Å and a long axis of 5.22 Å (5.30 Å if c of M- is considered). These lattice values are more comparable to either the T- or the M-phase with a short a and long c preferred in plane, but still, a mixture of C-/T-/M-phase is likely present. The results show that regardless of the crystalline phase, our Sr:HfO_2 films can accommodate both a short axis and a longer axis in plane. The long axis can correspond to the c-oriented T-phase and/or the b-/c-oriented M-phase. According to theoretical and experimental studies, such a phenomenon might occur when an in-plane tensile stress is produced on the films by the substrate.[9,33] Therefore, the transformation of $(001)_C/(100)_T$ to $(002/020)_M$ could be due to some form of tensile in-plane

https://doi.org/10.1021/acsaelm.3c01725
ACS Appl. Electron. Mater. 2024, 6, 1809−1820

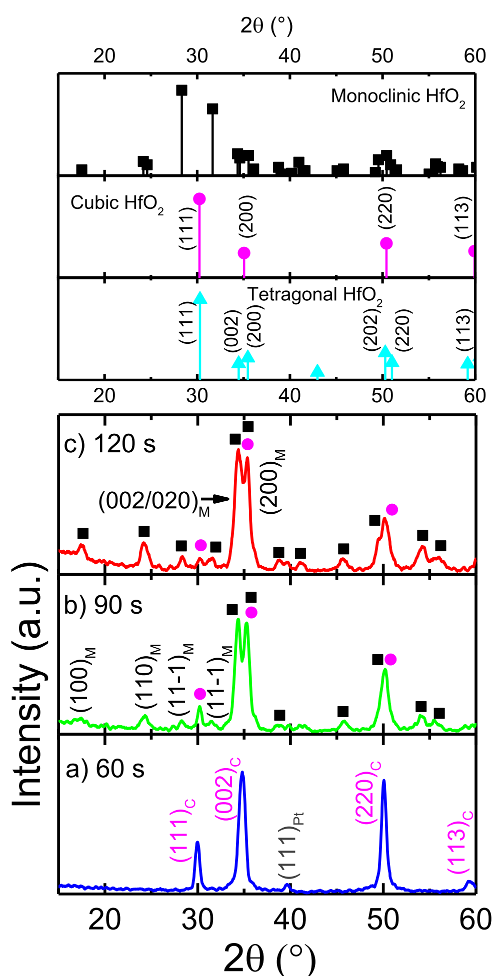

Figure 4. Standard X-ray reflections for powdered HfO_2 of monoclinic, cubic, and tetragonal phase (up). Fully in-plane θ–2θ X-ray diffraction measurements (down) with a grazing ω angle of 0.5° for Sr:HfO_2 samples annealed at 800 °C for (a) 60, (b) 90, and (c) 120 s. For simplicity, pink dots of the cubic phase are used to also denote diffraction planes of the tetragonal structure.

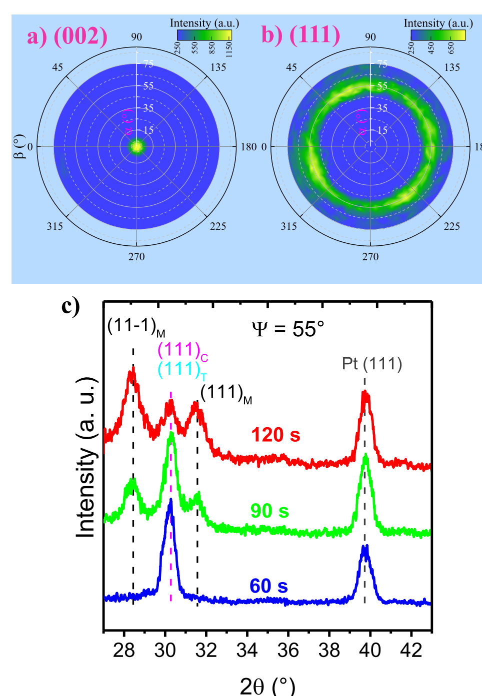

Figure 5. Polar figures for (a) $(002)_C/(200)_T$ and (b) $(111)_C/(111)_T$ reflections of a Sr:HfO_2 film annealed for 60 s at 800 °C. (c) Asymmetrical θ–2θ X-ray diffraction measurements at Ψ = 55° for Sr:HfO_2 films annealed for 60 (blue line), 90 (green), and 120 s (red) at 800 °C.

strain between our Sr:HfO_2 film and the bottom Pt(111) layer, which develops at some point during fabrication and/or thermal processing. This orientation arrangement allows for the longer b/c-axis of the monoclinic phase to expand mainly out of plane during annealing.

Interestingly, X-ray measurements at different rotation angles around the surface normal produced the same reflections. This invariance suggested that our films display a fiber texture with a strong $(001)_C/(100)_T$ preferential orientation out of plane (for 60 s of annealing) but a semirandom orientation in plane. This can be visualized as transversally structured columns with a unique orientation parallel to the surface normal but largely varying orientations perpendicular to the surface normal. We were able to experimentally verify the fiber texture by realizing polar figure measurements for the sample with 60 s of annealing. The results on fixing θ–2θ at 35.1° (for $(002)_C/(200)_T$) whereas tilting Ψ (α in polar figures) away from the normal surface while rotating the sample in φ (β in polar figures) from 0 to 360° are displayed in Figure 5a.[9] The observation of an intense diffraction dot at α = 0° (Ψ = 0°) can be regarded as orientation confirmation of the $(001)_C/(100)_T$ preferential crystallization out of plane. Further proof of the fiber texture was obtained by scanning for $(111)_C/(111)_T$ at fixed θ–2θ = 30.2° (Figure 5b). The intense Debye ring occurring at α = 55° is a further ratification of the $(001)_C/(100)_T$ orientation out of plane but also a corroboration of an in-plane semirandom $(111)_C/(111)_T$ orientation.[9] Taking advantage of the polar measurement configuration, we performed asymmetrical θ–2θ measurements at Ψ = 55° (α = 55° away from the surface normal).[9] At such a position, the {111} family of planes of either M- or C-/T-phases should appear with enough resolution, for an oriented film, to confirm the proportional presence of low-symmetry (M-) or high-symmetry (C-/T-) structures. As observed in corresponding Figure 5c, an evident C-/T- to M-phase transformation is observed as the annealing time is increased. This is deduced from the decrease in $(111)_{C,T}$ intensity while the $(11-1)_M$ and $(111)_M$ increase with annealing time. The lack of {002} reflections at around 2θ = 35° when Ψ = 55° is yet another proof of the preferential orientation of the films. A rough estimation of the composition of C-/T-phase in M-phase from Figure 5c was made by following the approximation of Nakayama et al. for {111} family of planes.[34] Compositions of 100, 55, and 26% of high symmetry oriented-C-/T-phases were calculated for Sr:HfO_2 films annealed at 800 °C for 60, 90, and 120 s, respectively. The same approximation was used to calculate the composition of the randomly oriented fraction from GI-XRD measurements (Figure 3) at ω = 0.55° (the {111} family of planes is less affected by orientation at such a low angle). Values of 100, 52, and 22% of C-/T-phase composition were found for 60, 90, and 120 s of annealing, respectively. The similarity in composition of the oriented and polycrystalline phases is consistent. It is expected, however, that the C-/T-phase-oriented fraction would benefit more from wake-up cycling. In our Sr:HfO_2 films, composed of three

https://doi.org/10.1021/acsaelm.3c01725
ACS Appl. Electron. Mater. 2024, 6, 1809−1820

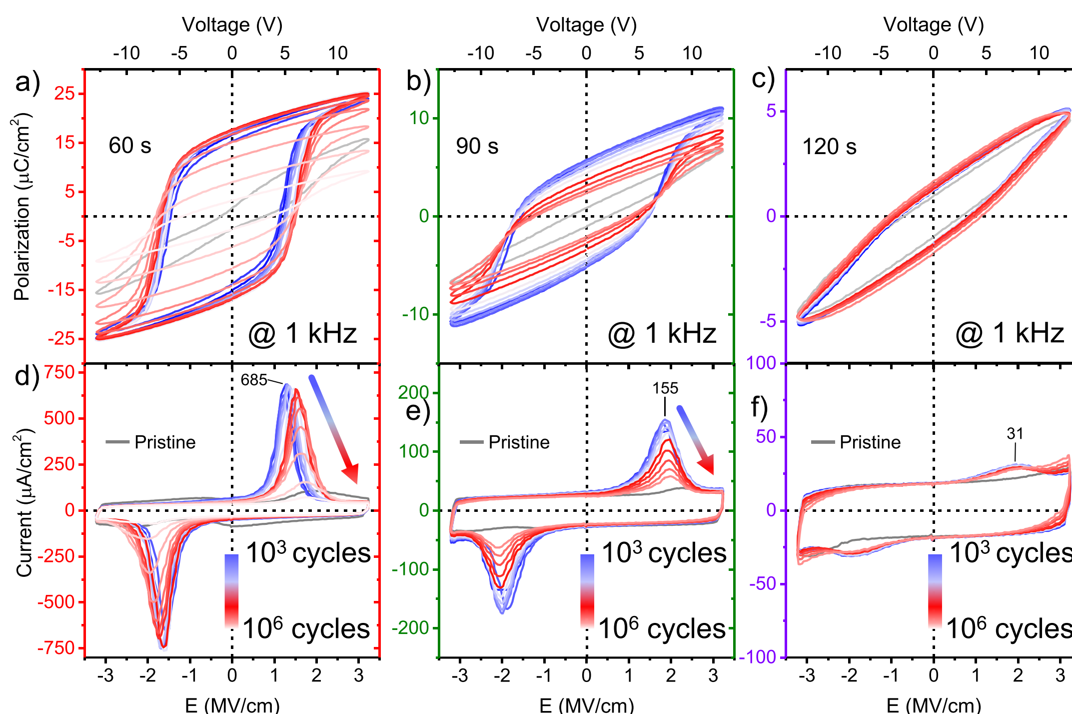

Figure 6. Field cycling behavior of polarization and transient current density loops from Sr:HfO_2 films annealed at 800 °C for 60 (a,d), 90 (b,e), and 120 s (c,f). Measurements were made under a fatigue load of 3.75 MV/cm at 1 kHz. Note that, for better observation, the *y*-scales are different for each image.

layers each, the newly deposited layers seem to follow the orientation of the layers below. It seems that the orientation of the films is pre-established during the pyrolysis process at 300 °C and largely enhanced during the rapid thermal annealing at 800 °C. In addition, even though we found evidence of a small fraction of randomly oriented HfO_2 crystals, the films are evidently highly $(001)_C/(100)_T$ oriented out of plane. It is also known, however, that next to phase transformation, reorientation in HfO_2 can take place depending on processing conditions during fabrication, annealing, and even electrical cycling.[14] This will be further investigated in a latter section.

Strong Ferroelectric Wake-Up in $(001)_C/(100)_T$ Oriented Sr:HfO_2. As is common in HfO_2-based films, the ferroelectric behavior usually develops or increases after the application of wake-up electrical cycling. This has been attributed to different factors, such as redistribution of oxygen vacancies, depinning of domains, and phase transformation to increase the volume ratio of polar orthorhombic structure.[35] As stated in the Experimental Details section, the Sr:HfO_2 films in this paper were woken up by rectangular pulses of 3.75 MV/cm at 1 kHz. The electrical cycling was maintained until ferroelectric fatigue took place. The films presented a degree of wake-up and fatigue that depended on the annealing time. Figure 6 displays the result of continuously applying electrical pulses at a frequency of 1 kHz. Initially, a pinched hysteresis loop is observed for the $(001)_C/(100)_T$-oriented Sr:HfO_2 film annealed at 800 °C for 60 s (Figure 6a). However, an intense wake-up effect is produced immediately upon application of the electrical pulses.[36] The ferroelectric response is maintained for a while, but the polarization loop eventually closes. In the end, only the polarization response typical of a dielectric material remains. These observations are even more apparent in the transient current density loops of the corresponding Figure 6d. Strong switching peaks are found right after wake-up cycling. Initially, the coercive fields are −1.74 and +1.5 MV/cm. Nevertheless, along with a decrease in switching currents, the coercive fields increase with continued electrical load. Additionally, despite the loss of ferroelectric response, no significant signs of leakage increase are detected.[26] This contrasts our previous work on Ca:HfO_2, where prolonged wake-up caused increased leakage for a thicker film of 54 nm. However, the first effects of fatigue appeared for a higher number of cycles in the Ca-doped films.[18]

Despite the loss of ferroelectric response already at 5×10^5 cycles for the Sr:HfO_2 films, their high remnant polarization and their good dielectric quality make it possible to study and distinguish the mechanisms giving origin to wake-up and fatigue. As discussed previously, the wake-up achieved for a $(001)_C/(100)_T$-oriented Sr:HfO_2 film annealed for 90 s at 800 °C was limited (Figure 6b). In this case, the ferroelectric response was lost even earlier, yet with no evidence of a leakage increase (Figure 6e). However, the coercive fields remained almost constant at −2.0 and +1.85 MV/cm. For the $(001/010)_M$-oriented Sr:HfO_2 film annealed for 120 s, the wake-up cycling had a minimal effect, and almost only dielectric behavior, with negligible leakage, was observed.

Now, we aim to relate the ferroelectric behavior of Figure 6 to the microstructural nature of the Sr:HfO_2 films observed in Figures 2 and 3. First, our results show that the ferroelectric phase, likely O-*Pca*2_1, might be initially present in pristine samples or produced/enhanced during wake-up cycling. Second, the extent of the ferroelectric behavior is related to the phase fraction that can acquire the polar O-phase structure. And third, the preferential orientation component also plays a role.[9,14] Commonly, the O-phase is reported to originate from a tetragonal-to-orthorhombic transformation.[31,32,37] Nevertheless, evidence of at least a partial transition from C- to O-phase has also been described in the literature, which has been

https://doi.org/10.1021/acsaelm.3c01725
ACS Appl. Electron. Mater. 2024, 6, 1809−1820

explained based on a redistribution of oxygen vacancies within the layers and instability of the cubic phase that transitions into the tetragonal phase.[12,32,36]

Considering the interplanar out-of-plane distances in our samples annealed for 60 s, a corresponding cubic or tetragonal out-of-plane lattice parameter is 5.07 Å (Table 1b). The calculated value indicates that the short *c*/*b* axis of the polar O-phase could be achieved in our films through a phase transformation.[15] Therefore, $(001)_O$ and $(010)_O$ orientations out of plane would be attained. Nevertheless, as the $(010)_O$ *b*-axis is perpendicular to the ferroelectric polarization, only the $(001)_O$-oriented grains of the O-phase would contribute to the ferroelectric switching response.[31] For our films, with a P_r of 17 $\mu C/cm^2$, in-plane tensile stress (forcing the long *a*-axis of O-in-plane) plays a role. Therefore, assuming a complete transformation to O-phase with the grains oriented with either *c* or *b*-axis out of plane (50% each), the maximum attainable P_r would be 28.5 $\mu C/cm^2$ (half of the theoretical value of 57 $\mu C/cm^2$).[9] The achievable value is considerably higher than our experimental one. Yet, various other considerations that decrease the P_r need to be contemplated, such as contamination with amorphous fractions and small-nuclei M-phase, random orientation of a portion of the grains (as indeed determined for our films), tilting of crystals away from the out-of-plane direction, the incomplete phase transformation from C-/T- to O-phase, and pinning of domains by defects.[12,38] For our remaining samples with annealing at 90 and 120 s, the lattice parameter out of plane increases to 5.16 Å (if the *b*-axis of M-phase is considered), which is no longer compatible with the short *b*- or *c*-axis of the O-phase. Both *b* and *c* of the M-phase unit cell are bigger than *a* and *c* of C- and T-unit cells (Table 1a), so if the transformation to *b* or *c* of M-phase occurs, it will cause increase of the cell volume.[31] The expansion also triggers in-plane stress because either *b*- or *c*-axis of M-phase grows perpendicularly to the film's normal, with some stress released upward. This release mechanism could explain why the *b*-oriented and *c*-oriented directions of M-phase are preferred out of plane, instead of shorter *a*. We also observed, as generally reported in the literature, that once a stable M-phase is attained, it cannot be transformed back into a polar O-phase by simple means.

Ferroelectric Fatigue in Sr:HfO_2 Films. To evaluate the electrical response and endurance of our Sr:HfO_2 films, fatigue testing with rectangular pulses of 3.75 MV/cm was made at different frequencies (Figure 7). For all frequencies above 1 kHz, ferroelectric wake-up was first performed at 1 kHz for 10^3 cycles. As evidenced in Figure 7a for Sr:HfO_2 annealed for 60 s, the endurance was higher for higher frequencies. Some other reports have shown that sustained high fields lead to faster fatigue.[39] Despite using 100 kHz, the ferroelectric endurance of our Sr:HfO_2 films was limited to less than 10^6 cycles. Interestingly, the electrical tests produced a loss of ferroelectric response but not an increase in leakage (evidenced as an artificial increase in P_r after ferroelectric fatigue).[18] The fatigue occurred sooner for an Sr:HfO_2 film annealed for 90 s (Figure 7b). Surprisingly, even if no signs of leakage were found during electrical cycling, all tested electrodes suffered from sudden hard breakdown for the sample annealed for 90 s. The breakdown was observed as burnt and broken electrodes. Such failure happened faster for lower frequencies, indicating that these devices were more sensitive to Joule heating. It was shown from Figure 5c that an almost 50/50 mixture of C-/T- and M-phases is present in films for this annealing time. All

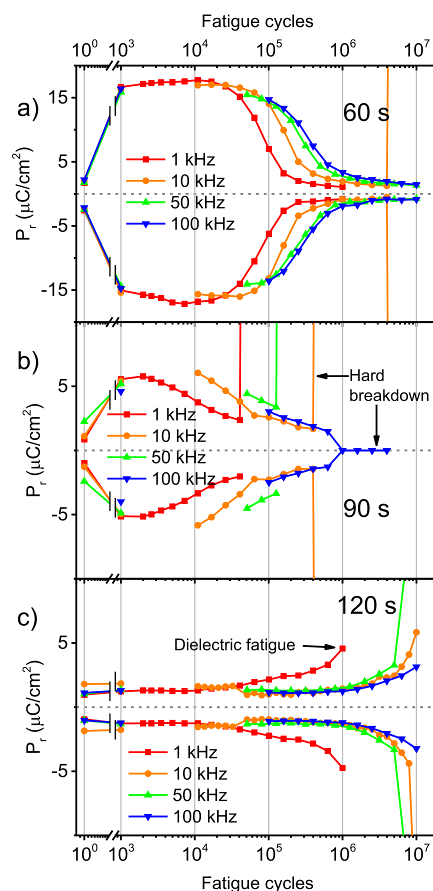

Figure 7. Fatigue behavior at different frequencies for Sr:HfO_2 films annealed for (a) 60, (b) 90, and (c) 120 s. The electrical load was 3.75 MV/cm. Note that the *y*-scale for (b,c) is smaller for ease of observation.

such phases have vastly different dielectric constants, and the mixture might result in an electrically inhomogeneous system with intense local fields, as observed by Schenk et al.[9] This is consistent with the behavior of a Sr:HfO_2 film annealed for 120 s (Figure 7c), which showed negligible ferroelectric wake-up but sustained the electric load with less evidence of sudden hard breakdown. For such a film, the M-phase was found to be most prominent (74%). In this case, nevertheless, a more common increase of leakage during wake-up cycling was finally observed, which might be related to the chemical and structural properties of the M-phase of HfO_2 when subject to continuous loads.

The most important result of wake-up and fatigue testing for our films is that the ferroelectric response of Sr:HfO_2 films annealed for 60 s was high initially, but it was lost relatively fast ($<10^6$ cycles). Yet, dielectric fatigue (leakage) was not found. Nevertheless, the conditions during prolonged electrical load favored the loss of the ferroelectric response, while maintaining a good insulating quality. A similar fatigue behavior of Sr:HfO_2 films (10 nm), but with higher endurance ($>10^8$ cycles) and P_r of 23 $\mu C/cm^2$, was reported by Schenk et al. for ALD-deposited films on TiN.[40] In the following section, we investigate the origin of the rapid fatigue of Sr:HfO_2.

Continuous Phase Transformation during Ferroelectric Operation. Capacitance−voltage measurements (CVM) were performed on a Sr:HfO_2 film annealed for 60 s to study the phenomena that gave rise to ferroelectric fatigue

https://doi.org/10.1021/acsaelm.3c01725
ACS Appl. Electron. Mater. 2024, 6, 1809−1820

during wake-up cycling. The relative dielectric constant (ε_r) was calculated by assuming a perfect parallel-plate capacitor. To avoid a cumulative effect of fatigue induced by long DC testing on a singularly tested electrode,[39] several individual electrodes of 200 μm diameter were instead woken up at 5 kHz and 3.25 MV/cm, fatigued for 5×10^3, 10^4, 10^5, or 10^6 cycles, before being subjected to CVM. The maximum field strength during CVM testing was 2.5 MV/cm. The dielectric constant behavior extracted from these measurements on a pristine electrode, in Figure 8a, shows an almost closed loop with an ε_r

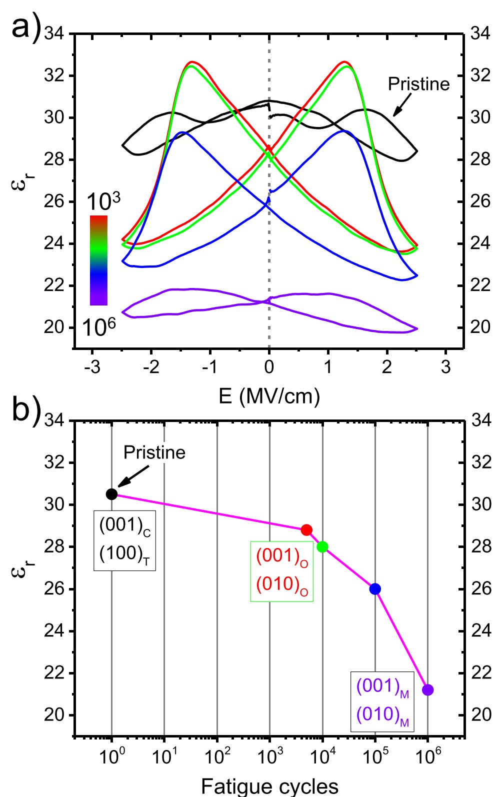

Figure 8. (a) Capacitance−voltage measurements of a ferroelectric $Sr{:}HfO_2$ film annealed for 60 s, fatigued at 5 kHz for an increasing number of cycles, and (b) effect on dielectric constant with prolonged fatigue cycling. Orientations in (b) denote the inferred phases and preferred orientations.

value around 30.5. This high value indicates a high-symmetry phase for HfO_2, which should be cubic or tetragonal, in agreement with the XRD analysis. Remarkably, the reported values of ε_r for T-HfO_2 are above 45;[31,33] thus, the observed reduced value points out to a mixture of C-, T-, and O-phases in pristine $Sr{:}HfO_2$ films which, after wake-up for 1×10^4 cycles, develops the characteristic loop of ferroelectric HfO_2 with an ε_r = 28.8 at 0 bias.

The ferroelectric wake-up with a slight drop in dielectric constant is likely due to conversion of a larger number of crystallites to the polar O-phase.[31,33] However, a further decrease of ε_r is found for an increasing number of fatigue cycles (1×10^5). In addition, the shape of the characteristic ferroelectric loop becomes flatter until it is almost lost at 1×10^6 cycles. This indicates the loss of the ferroelectric response of $Sr{:}HfO_2$. In Figure 8b, also the change in the value of ε_r with fatigue cycling is depicted. Evidently, the $Sr{:}HfO_2$ film's dielectric constant decreases with repetitive electrical measurements, eventually reaching 21.2, which is around the value reported for the M-phase of HfO_2.[31] In the work of Schenk et al., measured ε_r values of 32, 28, and 20 were assigned to C-, O-, and M-phases, respectively.[9] Unlike us, they found such values in La:HfO_2 films under decreasing doping concentrations of La, which produced increasing amounts of the M-phase. Thus, it makes sense that the ferroelectric wake-up and fatigue observed in our $Sr{:}HfO_2$ films is due to a phase transformation from $(001)_C/(100)_T$ through polar $(001)/(010)_O$, reaching $(001)/(010)_M$ oriented phases out of plane.[38] According to Materlik et al., this can be due to the loss of stability of the polar phase because of the formation of compensated defects during fatigue testing.[41]

The phenomena of phase transformation in hafnia during prolonged electrical load has already been studied and discussed in the literature.[42] Nevertheless, depending on processing conditions and particularly on the chemistry of the electrodes, different effects are observed. Most commonly, a T- to polar O-phase conversion is reported,[31,43,44] which produces sharp decreases in ε_r during wake-up.[37] However, conversion of M- to polar O-phase due to the presence and redistribution of oxygen vacancies has also been evidenced for HfO_2 on TiN,[36,45] thus causing a moderate increase of ε_r. Due to M- and O-phase being close in volume and energy, interconversion from one to another is possible under the right oxygen vacancy conditions.[31,36,38,43,46] Yet, transformation from T-/O- to M-phase during wake-up cycling, accompanied by a concurrent decrease of P_r, was also observed by Fields et al. This was corroborated by X-ray and electrical permittivity studies.[37] Remarkably, this detrimental phenomenon is present strongly in MIM capacitors made with Pt but to a much smaller degree in HfO_2 films capped with TaN or W electrodes. A frequent explanation for this relates to the accumulation of oxygen vacancies at interfaces. These cannot be exchanged with the Pt, thus losing the stabilizing effect provided by the oxygen vacancies to O-HfO_2.[37,47] There is thus a component due to the chemistry of the interface. Apart from stabilization of the O-phase, the top electrode also provides contention of volume expansion, which helps to avoid undesirable phase transformation from polar O- to nonpolar M-phase. Because of this, films are typically annealed with predeposited top electrodes.[33,45] At this point, it is essential to emphasize that our $Sr{:}HfO_2$ films are annealed without top electrodes. The top Pt contacts are deposited after annealing, and they are heated to at most 100 °C for a few minutes to improve adhesion. Therefore, it would be possible that higher endurance can be achieved by thermally processing the whole MIM stack together or replacing the material of the contacts. Work is ongoing to test if the HfO_2 films would also grow with the preferential (001) orientation.

■ CONCLUSIONS

We have used a simple and effective chemical solution deposition (CSD) approach to produce Sr (7.5 at. %):HfO_2 films with a record-high P_r of 17.3 μm/cm^2 for this dopant with this synthesis method and negligible leakage current. The strong ferroelectric wake-up was attained for films that originated from (001)/(100)-oriented cubic/tetragonal $Sr{:}HfO_2$ and were then annealed for 60 s at 800 °C. We believe that the remnant polarization value can be improved by further shortening of the annealing times. Longer annealing times produced a (001/010)-oriented monoclinic phase and greatly reduced remnant polarization values. In contrast to Ca

https://doi.org/10.1021/acsaelm.3c01725
ACS Appl. Electron. Mater. 2024, 6, 1809−1820

and other dopants used in CSD studies, HfO_2 doped with Sr requires shorter processing times. From XRD analysis and from electrical response during wake-up cycling, it is inferred that the (001)/(100)-oriented cubic/tetragonal phase undergoes a phase transformation to the orthorhombic phase with polar (001) and nonpolar (010)-orientations. Thus, the strong ferroelectricity found in our Sr:HfO_2 films can be explained by the generation of a large portion of favorably (001)-oriented orthorhombic crystals during electrical forming. However, an undesired continuous structural conversion to the nonpolar monoclinic phase occurs when electrical cycling is prolonged. This was made evident by a dielectric constant reduction from 30, in a pristine state, to 21 in fatigued capacitors. Although the current endurance of our films is limited to less than 10^6 cycles, there is ample room for optimization using different methods such as top electrode engineering. We consider our present work to be the first to show that crystal orientation control of HfO_2 films is possible via a simple chemical approach and subsequent processing. In addition, thin layer growth followed by layer-by-layer crystallization, as employed by Schenk et al., and tailoring of annealing atmosphere with leakage reduction, as done by Mandal et al., could improve the results further.[17,48] Moreover, our approach is compatible with methods aiming at fabricating thicker HfO_2 films[23,49] for NEMs and MEMs and promising for spray-coating and inkjet printing techniques for larger scale production.[50]

ASSOCIATED CONTENT

Supporting Information

The Supporting Information is available free of charge at https://pubs.acs.org/doi/10.1021/acsaelm.3c01725.

X-ray diffraction measurements in full θ–2θ geometry for Sr:HfO_2 films and substrate (PDF)

AUTHOR INFORMATION

Corresponding Authors

Beatriz Noheda – *Zernike Institute for Advanced Materials (ZIAM), Faculty of Science and Engineering, University of Groningen, 9747AG Groningen, The Netherlands; CogniGron (Groningen Cognitive Systems and Materials Center), University of Groningen, NL-9747 AG Groningen, Netherlands;* orcid.org/0000-0001-8456-2286; Email: b.noheda@rug.nl

Mónica Acuautla – *Engineering and Technology Institute Groningen (ENTEG), Faculty of Science and Engineering, University of Groningen, 9747AG Groningen, The Netherlands;* orcid.org/0000-0001-8763-8653; Email: m.i.acuautla.meneses@rug.nl

Authors

Miguel Badillo – *Engineering and Technology Institute Groningen (ENTEG), Faculty of Science and Engineering, University of Groningen, 9747AG Groningen, The Netherlands; Department of Physics, Politecnico di Milano, 20133 Milano, Italy;* orcid.org/0000-0002-2247-9222

Sepide Taleb – *Engineering and Technology Institute Groningen (ENTEG), Faculty of Science and Engineering, University of Groningen, 9747AG Groningen, The Netherlands;* orcid.org/0000-0002-0178-5925

Brenda Carreno Jimenez – *Engineering and Technology Institute Groningen (ENTEG), Faculty of Science and Engineering, University of Groningen, 9747AG Groningen, The Netherlands;* orcid.org/0000-0002-9805-8328

Taraneh Mokabber – *Engineering and Technology Institute Groningen (ENTEG), Faculty of Science and Engineering, University of Groningen, 9747AG Groningen, The Netherlands;* orcid.org/0000-0003-4911-5194

Rebeca Castanedo Pérez – *Centro de Investigación y de Estudios Avanzados del I.P.N. (CINVESTAV), Unidad Querétaro, 76230 Querétaro, Mexico;* orcid.org/0000-0002-2956-151X

Gerardo Torres-Delgado – *Centro de Investigación y de Estudios Avanzados del I.P.N. (CINVESTAV), Unidad Querétaro, 76230 Querétaro, Mexico;* orcid.org/0000-0001-7815-2774

Complete contact information is available at: https://pubs.acs.org/10.1021/acsaelm.3c01725

Author Contributions

The manuscript was written through contributions of all authors. All authors have given approval to the final version of the manuscript.

Notes

The authors declare no competing financial interest.

ACKNOWLEDGMENTS

We thank Jacob Baas, Henk Bonder, Marco Asa, and Joaquín Márquez for their technical support, as well as Prof. Sebastjan Glinsek and Barnik Mandal for fruitful discussion. We are also grateful to NanoLab and Polifab facilities and their staff at the University of Groningen and Politecnico di Milano. This work was supported by the start-up grant of the FSE at the University of Groningen, The Netherlands, and by a postdoctoral fellowship granted to Miguel Badillo (CVU 356403) by The National Council for the Humanities, Science and Technology (CONAHCYT), México. We also acknowledge the financial support of the CogniGron research center and the Ubbo Emmius Funds (Univ. of Groningen).

ABBREVIATIONS

PLD, pulsed laser deposition; ALD, atomic layer deposition; CSD, chemical solution deposition; XRD, X-ray diffraction; GI-XRD, grazing incidence X-ray diffraction; ICP, inductively coupled plasma; ICDD PDF, International Centre for Diffraction Data Powder Diffraction File

REFERENCES

(1) Matthews, J. N. A. Semiconductor Industry Switches to Hafnium-Based Transistors. *Phys. Today* **2008**, *61* (2), 25–26.

(2) Ohtaka, O.; Fukui, H.; Funakoshi, K.; Utsumi, W.; Irifune, T.; Kikegawa, T. Phase Relations and EOS of ZrO_2 and HfO_2 Under High-Temperature and High-Pressure. *High Pressure Res.* **2002**, *22* (1), 221–226.

(3) Böscke, T. S.; Müller, J.; Bräuhaus, D.; Schröder, U.; Böttger, U. Ferroelectricity in Hafnium Oxide Thin Films. *Appl. Phys. Lett.* **2011**, *99* (10), 102903.

(4) Barabash, S. V. Prediction of New Metastable HfO_2 Phases: Toward Understanding Ferro- and Antiferroelectric Films. *J. Comput. Electron.* **2017**, *16* (4), 1227–1235.

(5) Wei, Y.; Nukala, P.; Salverda, M.; Matzen, S.; Zhao, H. J.; Momand, J.; Everhardt, A. S.; Agnus, G.; Blake, G. R.; Lecoeur, P.; Kooi, B. J.; Íñiguez, J.; Dkhil, B.; Noheda, B. A Rhombohedral Ferroelectric Phase in Epitaxially Strained $Hf_{0.5}Zr_{0.5}O_2$ Thin Films. *Nat. Mater.* **2018**, *17* (12), 1095–1100.

(6) Starschich, S.; Boettger, U. An Extensive Study of the Influence of Dopants on the Ferroelectric Properties of HfO_2. *J. Mater. Chem. C* **2017**, *5* (2), 333−338.
(7) Hyuk Park, M.; Joon Kim, H.; Jin Kim, Y.; Lee, W.; Moon, T.; Seong Hwang, C. Evolution of Phases and Ferroelectric Properties of Thin $Hf_{0.5}Zr_{0.5}O_2$ Films According to the Thickness and Annealing Temperature. *Appl. Phys. Lett.* **2013**, *102* (24), 242905.
(8) Hoffmann, M.; Schroeder, U.; Schenk, T.; Shimizu, T.; Funakubo, H.; Sakata, O.; Pohl, D.; Drescher, M.; Adelmann, C.; Materlik, R.; Kersch, A.; Mikolajick, T. Stabilizing the Ferroelectric Phase in Doped Hafnium Oxide. *J. Appl. Phys.* **2015**, *118* (7), 072006.
(9) Schenk, T.; Fancher, C. M.; Park, M. H.; Richter, C.; Künneth, C.; Kersch, A.; Jones, J. L.; Mikolajick, T.; Schroeder, U. On the Origin of the Large Remanent Polarization in La:HfO_2. *Adv. Electron. Mater.* **2019**, *5* (12), 1900303.
(10) Batra, R.; Huan, T. D.; Rossetti, G. A.; Ramprasad, R. Dopants Promoting Ferroelectricity in Hafnia: Insights from a Comprehensive Chemical Space Exploration. *Chem. Mater.* **2017**, *29* (21), 9102−9109.
(11) Schroeder, U.; Yurchuk, E.; Müller, J.; Martin, D.; Schenk, T.; Polakowski, P.; Adelmann, C.; Popovici, M. I.; Kalinin, S. V.; Mikolajick, T. Impact of Different Dopants on the Switching Properties of Ferroelectric Hafnium Oxide. *Jpn. J. Appl. Phys.* **2014**, *53* (8S1), 08LE02.
(12) Schroeder, U.; Richter, C.; Park, M. H.; Schenk, T.; Pešić, M.; Hoffmann, M.; Fengler, F. P. G. G.; Pohl, D.; Rellinghaus, B.; Zhou, C.; Chung, C.-C.; Jones, J. L.; Mikolajick, T. Lanthanum-Doped Hafnium Oxide: A Robust Ferroelectric Material. *Inorg. Chem.* **2018**, *57* (5), 2752−2765.
(13) Shimizu, T.; Katayama, K.; Kiguchi, T.; Akama, A.; Konno, T. J.; Funakubo, H. Growth of Epitaxial Orthorhombic $YO_{1.5}$-Substituted HfO_2 Thin Film. *Appl. Phys. Lett.* **2015**, *107* (3), 032910.
(14) Shimizu, T.; Mimura, T.; Kiguchi, T.; Shiraishi, T.; Konno, T.; Katsuya, Y.; Sakata, O.; Funakubo, H. Ferroelectricity Mediated by Ferroelastic Domain Switching in HfO_2-Based Epitaxial Thin Films. *Appl. Phys. Lett.* **2018**, *113* (21), 212901.
(15) Katayama, K.; Shimizu, T.; Sakata, O.; Shiraishi, T.; Nakamura, S.; Kiguchi, T.; Akama, A.; Konno, T. J.; Uchida, H.; Funakubo, H. Orientation Control and Domain Structure Analysis of {100}-Oriented Epitaxial Ferroelectric Orthorhombic HfO_2-Based Thin Films. *J. Appl. Phys.* **2016**, *119* (13), 134101.
(16) Teng, C.-Y.; Cheng, C.-C.; Li, K.-S.; Hu, C.; Lin, J.-M.; Lin, B.-H.; Tang, M.-T.; Tseng, Y.-C. Optimizing the Ferroelectric Properties of $Hf_{1-X}Zr_xO_2$ Films via Crystal Orientation. *ACS Appl. Electron. Mater.* **2023**, *5* (2), 1114−1122.
(17) Schenk, T.; Bencan, A.; Drazic, G.; Condurache, O.; Valle, N.; Adib, B. E.; Aruchamy, N.; Granzow, T.; Defay, E.; Glinsek, S. Enhancement of Ferroelectricity and Orientation in Solution-Derived Hafnia Thin Films through Heterogeneous Grain Nucleation. *Appl. Phys. Lett.* **2021**, *118* (16), 162902.
(18) Badillo, M.; Taleb, S.; Mokabber, T.; Rieck, J.; Castanedo, R.; Torres, G.; Noheda, B.; Acuautla, M. Low-Toxicity Chemical Solution Deposition of Ferroelectric Ca:HfO_2. *J. Mater. Chem. C* **2023**, *11* (3), 1119−1133.
(19) Wei, A.; Chen, C.; Tang, L.; Zhou, K.; Zhang, D. Chemical Solution Deposition of Ferroelectric Sr:HfO_2 Film from Inorganic Salt Precursors. *J. Alloys Compd.* **2018**, *731*, 546−553.
(20) Tang, L.; Chen, C.; Wei, A.; Li, K.; Zhang, D.; Zhou, K. Regulating Crystal Structure and Ferroelectricity in Sr Doped HfO_2 Thin Films Fabricated by Metallo-Organic Decomposition. *Ceram. Int.* **2019**, *45* (3), 3140−3147.
(21) Yin, L.; Gong, S.; Li, X.; Lu, B.; Peng, Q.; Zheng, S.; Liao, M.; Zhou, Y. Improvement of Ferroelectricity and Endurance in Sr Doped $Hf_{0.5}Zr_{0.5}O_2$ Films. *J. Alloys Compd.* **2022**, *914*, 165301.
(22) Starschich, S.; Griesche, D.; Schneller, T.; Böttger, U. Chemical Solution Deposition of Ferroelectric Hafnium Oxide for Future Lead Free Ferroelectric Devices. *ECS J. Solid State Sci. Technol.* **2015**, *4* (12), P419−P423.
(23) Schenk, T.; Godard, N.; Mahjoub, A.; Girod, S.; Matavz, A.; Bobnar, V.; Defay, E.; Glinsek, S. Toward Thick Piezoelectric HfO_2-Based Films. *Phys. Status Solidi RRL* **2020**, *14* (3), 1900626.
(24) Franco-Linton, B.; Castanedo-Pérez, R.; Torres-Delgado, G.; Márquez-Marín, J.; Zelaya-Ángel, O. Influence of Vacuum and Ar/CdS Atmospheres-Rapid Thermal Annealing (RTA) on the Properties of Cd_2SnO_4 Thin Films Obtained by Sol-Gel Technique. *Mater. Sci. Semicond. Process.* **2016**, *56*, 302−306.
(25) Nagao, K.; Kagami, E. X-Ray Thin Film Measurement Techniques: VII. Pole Figure Measurement. *Rigaku J.* **2011**, *27* (2), 6−14.
(26) Schenk, T.; Yurchuk, E.; Mueller, S.; Schroeder, U.; Starschich, S.; Böttger, U.; Mikolajick, T. About the Deformation of Ferroelectric Hystereses. *Appl. Phys. Rev.* **2014**, *1* (4), 041103.
(27) Mimura, T.; Shimizu, T.; Kiguchi, T.; Akama, A.; Konno, T. J.; Katsuya, Y.; Sakata, O.; Funakubo, H. Effects of Heat Treatment and in Situ High-Temperature X-Ray Diffraction Study on the Formation of Ferroelectric Epitaxial Y-Doped HfO_2 Film. *Jpn. J. Appl. Phys.* **2019**, *58*, SBBB09.
(28) El-Shanshoury, I. A.; Rudenko, V. A.; Ibrahim, I. A. Polymorphic Behavior of Thin Evaporated Films of Zirconium and Hafnium Oxides. *J. Am. Ceram. Soc.* **1970**, *53* (5), 264−268.
(29) MacLaren, I.; Ras, T.; MacKenzie, M.; Craven, A. J.; McComb, D. W.; De Gendt, S. Texture, Twinning, and Metastable "Tetragonal" Phase in Ultrathin Films of HfO_2 on a Si Substrate. *J. Electrochem. Soc.* **2009**, *156* (8), G103.
(30) Muller, J.; Boscke, T. S.; Schroder, U.; Hoffmann, R.; Mikolajick, T.; Frey, L. Nanosecond Polarization Switching and Long Retention in a Novel MFIS-FET Based on Ferroelectric HfO_2. *IEEE Electron Device Lett.* **2012**, *33* (2), 185−187.
(31) Materlik, R.; Kunneth, C.; Kersch, A. The Origin of Ferroelectricity in $Hf_{1-X}Zr_xO_2$: A Computational Investigation and a Surface Energy Model. *J. Appl. Phys.* **2015**, *117* (13), 134109.
(32) Yuan, J.; Mao, G.; Xue, K.; Bai, N.; Wang, C.; Cheng, Y.; Lyu, H.; Sun, H.; Wang, X.; Miao, X. Ferroelectricity in HfO_2 from a Coordination Number Perspective. *Chem. Mater.* **2023**, *35* (1), 94−103.
(33) Fields, S. S.; Cai, T.; Jaszewski, S. T.; Salanova, A.; Mimura, T.; Heinrich, H. H.; Henry, M. D.; Kelley, K. P.; Sheldon, B. W.; Ihlefeld, J. F. Origin of Ferroelectric Phase Stabilization via the Clamping Effect in Ferroelectric Hafnium Zirconium Oxide Thin Films. *Adv. Electron. Mater.* **2022**, *8* (12), 2200601.
(34) Nakayama, S.; Funakubo, H.; Uchida, H. Crystallization Behavior and Ferroelectric Property of HfO_2-ZrO_2 Films Fabricated by Chemical Solution Deposition. *Jpn. J. Appl. Phys.* **2018**, *57*, 11UF06.
(35) Starschich, S.; Menzel, S.; Böttger, U. Evidence for Oxygen Vacancies Movement during Wake-up in Ferroelectric Hafnium Oxide. *Appl. Phys. Lett.* **2016**, *108* (3), 032903.
(36) Pešić, M.; Fengler, F. P. G.; Larcher, L.; Padovani, A.; Schenk, T.; Grimley, E. D.; Sang, X.; LeBeau, J. M.; Slesazeck, S.; Schroeder, U.; Mikolajick, T. Physical Mechanisms behind the Field-Cycling Behavior of HfO_2-Based Ferroelectric Capacitors. *Adv. Funct. Mater.* **2016**, *26* (25), 4601−4612.
(37) Fields, S. S.; Smith, S. W.; Ryan, P. J.; Jaszewski, S. T.; Brummel, I. A.; Salanova, A.; Esteves, G.; Wolfley, S. L.; Henry, M. D.; Davids, P. S.; Ihlefeld, J. F. Phase-Exchange-Driven Wake-Up and Fatigue in Ferroelectric Hafnium Zirconium Oxide Films. *ACS Appl. Mater. Interfaces* **2020**, *12* (23), 26577−26585.
(38) Rushchanskii, K. Z.; Blügel, S.; Ležaić, M. Ordering of Oxygen Vacancies and Related Ferroelectric Properties in $HfO_{2-\delta}$. *Phys. Rev. Lett.* **2021**, *127* (8), 087602.
(39) Starschich, S.; Menzel, S.; Böttger, U. Pulse Wake-up and Breakdown Investigation of Ferroelectric Yttrium Doped HfO_2. *J. Appl. Phys.* **2017**, *121* (15), 154102.
(40) Schenk, T.; Mueller, S.; Schroeder, U.; Materlik, R.; Kersch, A.; Popovici, M.; Adelmann, C.; Van Elshocht, S.; Mikolajick, T. Strontium Doped Hafnium Oxide Thin Films: Wide Process Window for Ferroelectric Memories. In 2013 Proceedings of the European

Solid-State Device Research Conference (ESSDERC); IEEE 2013, 260−263

(41) Materlik, R.; Künneth, C.; Mikolajick, T.; Kersch, A. The Impact of Charge Compensated and Uncompensated Strontium Defects on the Stabilization of the Ferroelectric Phase in HfO_2. *Appl. Phys. Lett.* **2017**, *111* (8), 082902.

(42) Lederer, M.; Abdulazhanov, S.; Olivo, R.; Lehninger, D.; Kämpfe, T.; Seidel, K.; Eng, L. M. Electric Field-Induced Crystallization of Ferroelectric Hafnium Zirconium Oxide. *Sci. Rep.* **2021**, *11* (1), 22266.

(43) Grimley, E. D.; Schenk, T.; Sang, X.; Pešić, M.; Schroeder, U.; Mikolajick, T.; LeBeau, J. M. Structural Changes Underlying Field-Cycling Phenomena in Ferroelectric HfO_2 Thin Films. *Adv. Electron. Mater.* **2016**, *2* (9), 1600173.

(44) Tashiro, Y.; Shimizu, T.; Mimura, T.; Funakubo, H. Comprehensive Study on the Kinetic Formation of the Orthorhombic Ferroelectric Phase in Epitaxial Y-Doped Ferroelectric HfO_2 Thin Films. *ACS Appl. Electron. Mater.* **2021**, *3* (7), 3123−3130.

(45) Choi, J. C.; Song, M. S.; Lee, K.; Park, K.; Park, J.; Lee, H.; Lee, J. H.; Chae, S. C. Dynamic Analysis of Non-Linear Wake-up Behavior in $Hf_{0.7}Zr_{0.3}O_2$ Thin Film. *Curr. Appl. Phys.* **2020**, *20* (6), 746−750.

(46) Nittayakasetwat, S.; Kita, K. Evidence of Ferroelectric HfO_2 Phase Transformation Induced by Electric Field Cycling Observed at a Macroscopic Scale. *Solid-State Electron.* **2021**, *184*, 108086.

(47) Fields, S. S.; Smith, S. W.; Fancher, C. M.; Henry, M. D.; Wolfley, S. L.; Sales, M. G.; Jaszewski, S. T.; Rodriguez, M. A.; Esteves, G.; Davids, P. S.; McDonnell, S. J.; Ihlefeld, J. F. Metal Nitride Electrode Stress and Chemistry Effects on Phase and Polarization Response in Ferroelectric $Hf_{0.5}Zr_{0.5}O_2$ Thin Films. *Adv. Mater. Interfaces* **2021**, *8* (10), 2100018.

(48) Mandal, B.; Valle, N.; Abid, B. E.; Girod, S.; Menguelti, K.; Defay, E.; Glinsek, S. Control of Ferroelectricity in Solution-Processed Hafnia Films through Annealing Atmosphere, 2024, manuscript under review.

(49) Mimura, T.; Shimizu, T.; Funakubo, H. Ferroelectricity in $YO_{1.5}$-HfO_2 Films around 1μm in Thickness. *Appl. Phys. Lett.* **2019**, *115* (3), 032901.

(50) Godard, N.; Glinšek, S.; Matavž, A.; Bobnar, V.; Defay, E. Direct Patterning of Piezoelectric Thin Films by Inkjet Printing. *Adv. Mater. Technol.* **2019**, *4* (2), 1800168.

https://doi.org/10.1021/acsaelm.3c01725
ACS Appl. Electron. Mater. 2024, 6, 1809−1820